Structural and Optical Properties of Passivated Silicon Nanoclusters with Different Shapes: A Theoretical Investigation

Bo-Cheng Wang,*,† Yu-Ma Chou,‡ Jin-Pei Deng,† and Yu-Tsai Dung†

Department of Chemistry, Tamkang University, Tamsui 251, Taiwan, and Department of Physics, Chinese Culture University, Taipei 110, Taiwan

Received: January 23, 2008; Revised Manuscript Received: April 1, 2008

Optimized geometries and electronic structures of hydrogenated silicon nanoclusters, which include the T_d and I_h symmetries, have been generated by using the semiempirical AM1 and PM3 methods, the density functional theory (DFT) B3LYP method with the 6−31G(d) and LANL2DZ basis sets from the Gaussian 03 package, and the local density functional approximation (LDA), which is implemented in the SIESTA package. The calculated diameters for these T_d symmetric hydrogenated silicon nanoclusters are in the range from 6.61 Å (Si_5H_{12}) to 23.24 Å ($Si_{281}H_{172}$). For the I_h symmetry, we calculated $Si_{20}H_{20}$ and $Si_{100}H_{60}$ nanoclusters only. Theoretically, the energy gap between the highest occupied molecular orbital (HOMO) and the lowest unoccupied molecular orbital (LUMO) is size dependent. The calculated energy gap decreases (Si_5H_{12}: 7.65 eV to $Si_{281}H_{172}$: 3.06 eV) while the diameter of silicon nanocluster increases. By comparing different calculated results, we concluded that the calculated energy gap by B3LYP/6−31G(d)//LDA/SIESTA is close to that from experiment and that the LDA/SIESTA result underestimates the experimental value. On the contrary, the AM1 and PM3 results overestimate the experimental results. For investigation of the optical properties of Si nanoclusters as a function of surface passivation, we carried out a B3LYP/6−31G(d)//LDA/SIESTA calculation of the Si_{35} and Si_{47} core clusters with full alkyl-, OH−, NH_2−, CH_2NH_2−, OCH_3−, SH−, C_3H_6SH−, and CN− passivations. The calculated optical properties of alkyl passivated Si_{35} nanoclusters ($Si_{35}(CH_3)_{36}$, $Si_{35}(C_2H_5)_{36}$, and $Si_{35}(C_3H_7)_{36}$) are close to one another and are higher than those of oxide, nitride, and sulfide passivated Si_{35} clusters. In conclusion, the alkyl passivant affects weakly the calculated optical gaps, and the electron-withdrawing passivants generate a red-shift in the energy gap of silicon nanoclusters. A size-dependent effect is also observed for these passivated Si nanoclusters.

Introduction

Recently, the silicon nanocrystalline materials have become one of the most interesting topics in physics, chemistry, material science, and biophysics because of their diverse applications, such as for solar energy conversion, semiconductor nanomaterials in photography, quantum dot devices, and biomedical applications.[1–5] During the last decade, physical and chemical properties of nanocrystalline silicon have been studied intensively.[6–12] According to experiments and theoretical predictions, the properties of silicon clusters are size dependent and larger silicon clusters are close to bulk silicon material in optical properties. A large blue-shift is found in nanoclusters in the observed radiation with respect to the bulk Si band gap energy.[12]

At present, a limited amount of papers have been published on the theoretical treatments of optical properties of hydrogenated silicon nanoclusters, which include semiempirical modified neglet of diatomic overlap (MNDO), tight-binding, time-dependent density functional theory (TD-DFT), local density approximation (LDA), quantum Monte Carlo, and time-dependent local density approximation (TD-LDA) methods.[6,7,9,13–16] Reboredo et al. compared several calculated results with experimental data.[17] Vasiliev et al. computed the excitation energy for Si_nH_m clusters by using TD-DFT method.[7] Very recently, Wang et al. calculated absorption and emission energies of small hydrogenated silicon nanoclusters by the TD-DFT method.[18] Particularly, most of these calculations focus on the dependence of the energy gap on the size and shape of the silicon nanoclusters.

To improve the optical properties of hydrogenated Si nanoclusters, passivated Si nanoclusters with different passivation were generated by organic synthesis reactions.[5,19,20] The experimental results show that the passivated silicon nanocluster is an ideal candidate for biological fluorescence imaging without toxicology.[4,21] Recently, alkyl- and allylamine-passivated silicon nanoclusters were generated with simple organic syntheses by Warner et al. and Tanaka et al., respectively.[5,22] From a theoretical point of view, some organic groups may replace a single H atom at the surface of Si nanocluster which influences their optical properties.[23] Then, Zhou and co-workers used the static and TD-DFT calculations to investigate the optical properties of the core/shell nanoclusters with F− and OH− passivations.[24,25] Reboredo and Galli discussed the energy gap of silicon nanoclusters with reconstructed surfaces completed by alkyl passivation.[26] Vasiliev determined the excited-state properties of passivated silicon nanoclusters by the TD-DFT method.[27] In particular, the interplay between quantum confinement effect in the Si core and the extrinsic passivation effect is still unclear. To understand the cluster surface and to predict the passivation effect, theoretical calculations may be needed, which is one of the most promising tools to understand the optical properties of the passivated silicon nanoclusters.

* To whom correspondence should be addressed. Tel: +8862-26215656; ext 2533; fax: +8862-26209924; e-mail: bcw@mail.tku.edu.tw.
† Tamkang University.
‡ Chinese Culture University.

10.1021/jp8006975 CCC: $40.75
Published on Web 06/21/2008

Theoretically, an accurate quantum mechanics calculation is limited because of the large computation demand. Although a few papers have been published on the optical properties and electronic structures of hydrogenated silicon clusters with different symmetry, a systematic study for these clusters with different calculation methods is not available so far. In this paper, we determined more efficient calculation methods to predict the optical properties of silicon nanoclusters. The B3LYP method with the 6−31G(d) basis set and semiempirical (AM1 and PM3) calculations (Gaussian 03) are presented on the basis of the optimized structure by the local density approximation (LDA) in the SIESTA package.[29,13] These calculations are used to study the hydrogenated tetrahedral silicon clusters (i.e., Si_5H_{12}, $Si_{17}H_{36}$, $Si_{29}H_{36}$, $Si_{35}H_{36}$, $Si_{47}H_{60}$, $Si_{71}H_{108}$, $Si_{99}H_{100}$, $Si_{147}H_{148}$, and $Si_{281}H_{172}$) and their diameters ranging from 6.61 Å to 23.24 Å. For the I_h symmetric silicon nanoclusters, Zhao et al. predicted relative stability and physical properties of the hydrogenated silicon nanoclusters by first-principle calculations.[28] In the present paper, we attempted to study two hydrogenated icosahedral silicon nanoclusters $Si_{20}H_{20}$ and $Si_{100}H_{60}$ by the B3LYP method on the basis of the LDA optimized structure and also compared their properties to the optical properties of tetrahedral (T_d) silicon nanoclusters with the close core size. The aim of this study is to generate the size dependence of structural and optical properties in the hydrogenated silicon nanoclusters with T_d and I_h symmetries through different quantum mechanic calculations and to improve them with available calculations and related experimental data.

Functionalization of Si surface at the nanoclusters may give an opportunity to use them in the range of photonic applications, which include optical sensing techniques, biological fluorescence imaging, and optoelectronic devices.[4,5] In particular, most of the previous works have focused on the Si nanoclusters with different core sizes, and the data regarding the optical properties of passivated Si nanoclusters are still scarce. However, a few papers were published related to the theoretical and experimental studies on the passivated Si nanoclusters.[20–26] In this paper, the B3LYP and LDA calculations were carried out to determine the highest occupied molecular orbital (HOMO), lowest unoccupied molecular orbital (LUMO), energy gap, and Fermi energy for the fully passivated Si nanoclusters with different organic surface passivations, core sizes, and symmetries (i.e., $Si_{35}(OH)_{36}$, $Si_{35}(CH_3)_{36}$, $Si_{35}(C_2H_5)_{36}$, $Si_{35}(C_3H_7)_{36}$, $Si_{35}(C_2H_3)_{36}$, $Si_{35}(NH_2)_{36}$, $Si_{35}(CH_2NH_2)_{36}$, $Si_{35}(OCH_3)_{36}$, $Si_{35}[(CH_2)_3SH]_{36}$, $Si_{35}(CN)_{36}$, $Si_{47}(CH_3)_{60}$, $Si_{20}(CH_3)_{20}$, etc.). On the basis of these calculation results, we will discuss the connection between the optical properties and electronic structures of well-defined and defect-free passivated Si nanoclusters. The calculated density of states (DOS) and spectral properties of these passivated Si nanoclusters are also discussed.

Details of Computations. Si nanocrystalline particles may have T_d or I_h or other symmetries. Conventionally, the hydrogenated silicon cluster has T_d symmetry and contains the diamondlike tetravalent sp^3 bonding with a spherical shape and the surface-dangling bonds being terminated by H atoms. The simplest hydrogenated silicon cluster with T_d symmetry considered in this study is Si_5H_{12}; it contains the central Si atom bound with four silicon atoms by means of sp^3 hybridized orbitals. For the larger silicon cluster with T_d symmetry, the Si atoms are extended along the C_3 axes through the central Si atom (Figure 1). Recently, Zhao et al. predicted stable icosahedral silicon clusters with tetravalent bonding by using first-principle calculations; they do not contain a central Si atom and their shape and symmetry are very similar to those of the fullerene family.[28] Theoretically, the icosahedral silicon nanoclusters may be the other possibility existing for silicon clusters. The simplest core icosahedral silicon nanocluster is Si_{20}, which contains 12 pentagonal faces. The pentagons are extended along the C_5 axis in the larger silicon clusters with I_h symmetry. Since the tetravalent bonding should be maintained for the Si atom, the next possible I_h core silicon nanocluster is Si_{100}.

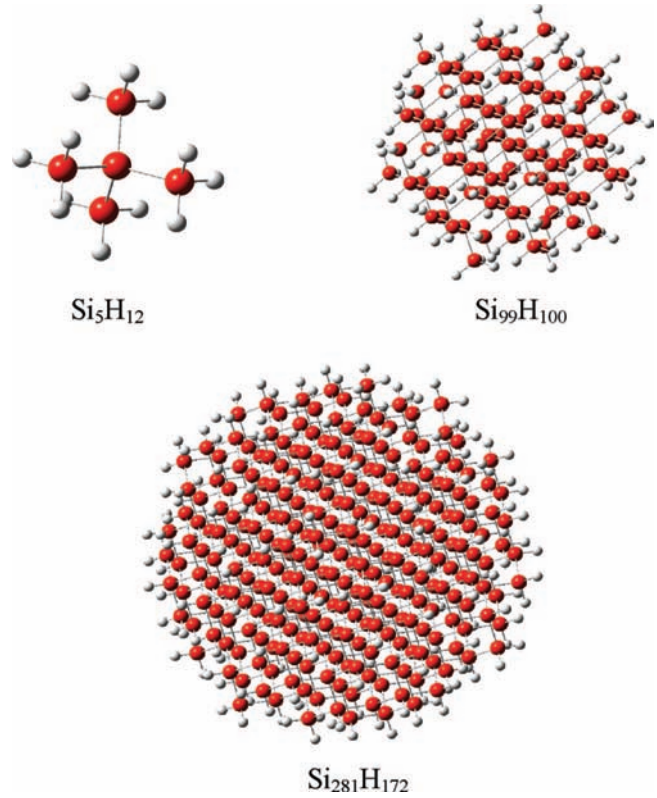

Figure 1. Optimized structures of Si_5H_{12}, $Si_{99}H_{100}$, and $Si_{281}H_{172}$.

Since the computational demands required for the silicon cluster calculations are large, an efficient calculation method is needed to investigate their physical properties. From the theoretical point of view, accurate ab initio and DFT calculations with large basis sets are too costly; most computers cannot calculate clusters with over 50 Si atoms. The aim of this study is to select an appropriate method for calculating large silicon clusters.

In this study, we employed a DFT-based method implemented in the SIESTA simulation package, which provides a very useful calculation technique for theoretical studies of periodical systems with a large number of atoms.[29] It uses the standard Kohn-Sham self-consistent density function method in the local density approximations (LDA) and generalized gradient approximation (GGA) with parameterization of Perdew and co-workers.[30] The basis set is a linear combination of numerical atomic orbitals (LCAO), which includes double-ξ polarized orbitals, where two s and three p orbitals for the H valence electron and two s, six p, and five d orbitals for the Si valence electrons were used, and the energy cutoff is 100 Ry to define the finite real-space grid. Actually, the supercell is generated automatically in these clusters; it is large enough for interaction between neighboring clusters to be negligible. Since the energy gap of a silicon cluster is size-dependent, we used the semiempirical AM1 and PM3 methods and DFT B3LYP with 6−31G(d) basis set to generate the electronic structure of silicon nanoclusters on the basis of the optimized structure of LDA/SIESTA; we denote this procedure by (method)/(basis set)//(functional)/SIESTA (method

TABLE 1: Calculated Energy Gap of Si_mH_n at Different Levels of Theory[a]

Si_mH_n	B3LYP/6−31G(d) // LDA/SIESTA	AM1// LDA/ SIESTA	PM3// LDA/ SIESTA	LDA/ SIESTA	B3LYP/ 6−31G(d)	AM1	PM3	B3LYP/ LANL2DZ
Si_5H_{12}	7.65	9.31	7.30	5.96	7.60	9.21	7.28	8.12
$Si_{17}H_{36}$	5.98 (5.98)[b]	8.32	6.08	4.42 (4.58)[c]	5.76	8.28	6.09	6.39
$Si_{29}H_{36}$	5.32 (5.33)[b]	7.85	5.60	3.67 (3.85)[c]	5.29	7.84	5.59	5.71
$Si_{35}H_{36}$	5.12 (5.14)[b]	7.73	5.43	3.56 (3.72)[c]	5.10	7.71	5.41	5.65
$Si_{47}H_{60}$	4.94 (4.96)[b]	7.62	5.25	3.40 (3.57)[c]		7.62	5.04	5.46
$Si_{71}H_{108}$	4.18	7.24	4.94	2.75		7.22	4.96	
$Si_{99}H_{100}$	3.95	7.03	4.66	2.52		7.02	4.66	
$Si_{147}H_{148}$	3.62	6.87	4.42	2.22				
$Si_{281}H_{172}$	3.06	6.58	4.06	1.69				

[a] Energy unit is eV. [b] The calculated energy gaps by B3LYP/6−31G(d)//GGA/SIESTA are indicated in parentheses. [c] The calculated energy gaps by GGA/SIESTA are indicated in parentheses.

TABLE 2: Calculated Si_mH_n (T_d) Nanocluster Diameter (Å) at Different Levels of Theory[a]

Si_mH_n	LDA/SIESTA	B3LYP /6−31G(d)	AM1	PM3	B3LYP/ LANL2DZ
Si_5H_{12}	6.61 (2.31)	6.70	6.67 (2.38)	6.71 (2.38)	6.68
$Si_{17}H_{36}$	10.28 (2.32)	10.61	10.31 (2.38)	10.49 (2.38)	10.08
$Si_{29}H_{36}$	11.24 (2.33)	11.60	11.59 (2.37)	11.61 (2.36)	11.55
$Si_{35}H_{36}$	11.60 (2.33)	12.70	12.79 (2.36)	12.29 (2.36)	13.77
$Si_{47}H_{60}$	14.12 (2.33)		15.55 (2.36)	15.47 (2.36)	15.92
$Si_{71}H_{108}$	14.93 (2.33)		14.98 (2.37)	16.09 (2.36)	
$Si_{99}H_{100}$	17.85 (2.33)		16.60 (2.35)	17.98 (2.34)	
$Si_{147}H_{148}$	20.66 (2.33)				
$Si_{281}H_{172}$	23.24 (2.34)				

[a] The calculated Si−Si bond lengths are indicated in parentheses.

is B3LYP, AM1, or PM3; functional is LDA or GGA). All the calculations were performed for T_d and I_h symmetries of Si nanoclusters. We also used the semiempirical AM1, PM3, and B3LYP/6−31G(d) methods as well as B3LYP/LANL2DZ pseudopotential, which treats the electron near the nucleus in an approximate way. Calculations to determine the optimized geometry and electronic structures were carried out by different methods for comparisons.

To investigate the passivation effect in the Si nanocluster, we explore alkyl, oxide, nitride, sulfide, and CN different passivants on the surface of Si clusters. The calculated HOMO, LUMO, and Fermi energy were generated by the B3LYP/6−31G(d)//LDA/SIESTA method. In principle, Fermi energy is $-(I + A)/2$; I (ionization potential) and A (electron affinity) correspond to the HOMO and LUMO for the Si nanoclusters, respectively, because of polarization energies and self-energy corrections.[24]

Semiempirical AM1 and PM3 and B3LYP/LANL2DZ and B3LYP/6−31G(d) geometry optimization were performed only up to $Si_{47}H_{60}$ and $Si_{35}H_{36}$ clusters because of the large calculation demands. The semiempirical AM1 and PM3 and B3LYP/6−31G(d) and B3LYP/LANL2DZ calculations were carried out using the Gaussian 03 package.[31]

Results and Discussion

In this study, the B3LYP method with the 6−31G(d) and LANL2DZ basis sets and the semiempirical AM1, PM3, and LDA methods were chosen to determine the electronic and geometrical structures of hydrogenated silicon nanoclusters including those with T_d and I_h symmetries. Because of computation limitations, we optimized the Si nanoclusters up to $Si_{281}H_{172}$ and $Si_{100}H_{60}$ with the T_d and I_h symmetries, respectively, using the SIESTA package. In Table 1, we summarized the LDA/SIESTA, B3LYP/6−31G(d)//LDA/SIESTA, AM1//LDA/SIESTA, PM3//LDA/SIESTA, B3LYP/6−31G(d), and B3LYP/LANL2DZ calculated energy gap of hydrogenated tetrahedral silicon nanoclusters ranging from Si_5H_{12} to $Si_{281}H_{172}$. We calculated the energy gap of silicon nanoclusters from Si_5H_{12} up to $Si_{35}H_{36}$, $Si_{99}H_{100}$, and $Si_{47}H_{60}$ by the B3LYP/6−31G(d), semiempirical (AM1, PM3), and B3LYP/LANL2DZ methods, respectively. According to Table 1, the B3LYP/6−31G(d)//LDA/SIESTA results are close to those of B3LYP/6−31G(d) calculations (7.65 eV vs 7.60 eV for Si_5H_{12}; 5.98 eV vs 5.76 eV for $Si_{17}H_{36}$; 5.12 eV vs 5.10 eV for $Si_{35}H_{36}$); the LDA/SIESTA method gives the smallest calculated energy gap as compared to the other methods. In fact, several papers have reported that the LDA approach is well-known to underestimate the experimental energy gap.[7,12,15] Garoufalis and Zdetsis et al. have determined the energy gap by using the B3LYP method with the [SV(P)] basis set; for comparison, our B3LYP/6−31G(d)//LDA/SIESTA results are about 0.1 eV higher than those by Garoufalis and Zdetsis.[13] The B3LYP calculation with the pseudopotential LANL2DZ basis set has also been used in this study. The B3LYP/LANL2DZ results are higher than those of B3LYP/6−31G(d) and B3LYP/6−31G(d)//LDA/SIESTA calculations since the pseudopotential LANL2DZ basis set treats the core electrons approximately and it may overestimate the calculated energy gap. The energy gaps are very close in the two sets of calculations, AM1//LDA/SIESTA and AM1, PM3//LDA/SIESTA, and PM3. Theoretically, the semiempirical (AM1 and PM3) methods are based on the neglect of diatomic differential overlap approximation (NDDO); these calculation results may be higher than those of B3LYP calculations. For comparison, the calculations with LDA/SIESTA, GGA/SIESTA, and single-point B3LYP calculations based on the optimized GGA/SIESTA geometries for limited hydrogenated Si nanoclusters were also carried out. There are slight differences in the calculated energy gap with GGA/SIESTA and LDA/SIESTA methods (Table 1).

Table 2 shows the calculated cluster size by different methods; the size of tetrahedral Si clusters considered in this study ranges

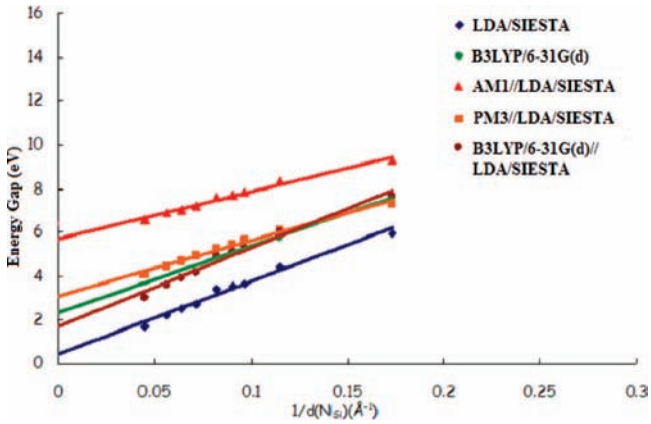

Figure 2. A plot of the calculated energy gap vs 1/d(N_{si}) for the silicon clusters.

from Si_5H_{12} to $Si_{281}H_{172}$. Zunger and Wang have proposed the equation for the diameter of Si core nanoclusters, which do not include any passivation on the cluster surface, as $d(N_{si}) = 3.3685N_{Si}^{1/3}$(Å) ($d(N_{si})$ and N_{si} are the calculated diameter of silicon nanocluster and the number of silicon atoms in the cluster, respectively.).[32] According to this table, the diameters calculated by LDA/SIESTA for the hydrogenated silicon nanoclusters range from 6.61 Å (Si_5H_{12}) to 23.24 Å ($Si_{281}H_{172}$). Comparing the calculated cluster diameters, those obtained by AM1, PM3, and B3LYP methods are very close and are smaller than that from LDA/SIESTA calculation. Since the tight-binding method assumes that all of the Si−Si bonds have the same length in the whole silicon cluster, the geometry cannot be optimized. The calculated average Si−Si bond lengths by different methods are from 2.31 Å to 2.34 Å, which is close to that in the bulk silicon material (2.35 Å).[15]

Several theoretical and experimental works mentioned that the energy gaps are cluster size dependent; the calculated energy gaps of silicon nanoclusters decrease while the size of clusters increases.[13–16] Thus, our calculation results are consistent with previous theoretical and experimental data. In Figure 2, we plotted the calculated energy gap versus 1/d(N_{si}), and the intercept is the energy gap for the bulk silicon material. Comparing the calculated approximate energy gap by different methods, the B3LYP/6−31G(d)//LDA/SIESTA value (1.70 eV) is the closest to that of bulk silicon (1.17 eV); the LDA/SIESTA energy (0.44 eV) is underestimated and the values of AM1//LDA/SIESTA (5.72 eV) and PM3//LDA/SIESTA (3.08 eV) are overestimated as compared to experiment.[33]

According to the above calculations, we can see that the Si nanoclusters exhibit the quantum confinement effect in these quantum dots. Their calculated energy levels are similar to that of a free particle in a cubic box [$(E_{n_x,n_y,n_z} = h^2/8ma^2(n_x^2+n_y^2+n_z^2))$, and a is the length of cubic box]. While a increases, E decreases, and thus the Si nanoclusters show the size dependence.

Among icosahedral silicon nanoclusters, we calculated optimized structures and the energy gap for the hydrogenated silicon cluster $Si_{20}H_{20}$ and $Si_{100}H_{60}$ by using the B3LYP/6−31G(d)//LDA/SIESTA method, and the results are shown in Figure 3 and Table 3, respectively. Comparing the calculated energy gap and the optimized cluster diameter of $Si_{99}H_{100}$ (T_d) and $Si_{100}H_{60}$ (I_h) clusters, we can see that they contain almost the same number of silicon atoms although their symmetries are different. The calculated energy gap of $Si_{100}H_{60}$ (I_h) is 0.53 eV lower than that of $Si_{99}H_{100}$ (T_d). Thus, the icosahedral Si

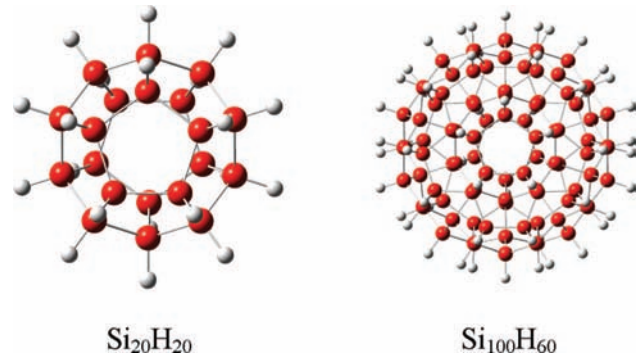

Figure 3. Optimized structures of $Si_{20}H_{20}$ and $Si_{100}H_{60}$.

TABLE 3: Calculated HOMO, LUMO, and Energy Gap (eV) of Icosahedral Nanoclusters

	B3LYP/6−31G(d)//LDA/SIESTA			
compounds	HOMO	LUMO	energy gap	Fermi energy
$Si_{20}H_{20}$	−6.83	−2.03	4.80	−4.43
$Si_{20}(CH_3)_{20}$	−5.34	−1.40	3.94	−3.37
$Si_{20}(OH)_{20}$	−5.44	−3.19	2.25	−4.16
$Si_{100}H_{60}$	−6.21	−2.79	3.42	−4.50
$Si_{100}(CH_3)_{60}$	−4.87	−1.49	3.38	−3.18

TABLE 4: Calculated HOMO, LUMO, and Energy Gap (eV) of Passivated Si Nanoclusters by B3LYP/6−31G(d)//LDA/SIESTA Method

	B3LYP/6−31G(d)//LDA/SIESTA			
compounds	HOMO	LUMO	energy gap	Fermi energy
$Si_{35}H_{36}$	−6.80	−1.68	5.12	−4.24
$Si_{35}(CH_3)_{36}$	−5.43	−0.83	4.60	−3.13
$Si_{35}(CH_2CH_3)_{36}$	−5.34	−0.75	4.59	−3.05
$Si_{35}(CH_2CH_2CH_3)_{36}$	−5.45	−0.75	4.70	−3.10
$Si_{35}(CH{=}CH_2)_{36}$	−5.34	−1.04	4.30	−3.19
$Si_{35}(OH)_{36}$	−5.60	−2.75	2.84	−4.18
$Si_{35}(NH_2)_{36}$	−4.13	−0.74	3.39	−2.44
$Si_{35}(CH_2NH_2)_{36}$	−3.61	−0.33	3.28	−1.97
$Si_{35}(OCH_3)_{36}$	−5.66	−2.43	3.23	−4.05
$Si_{35}(CN)_{36}$	−9.17	−4.65	4.52	−6.91
$Si_{35}(SH)_{36}$	−6.40	−2.99	3.41	−4.70
$Si_{35}[(CH_2)_3SH]_{36}$	−5.62	−1.22	4.40	−3.42
$Si_{47}(CH_3)_{60}$	−5.36	−0.92	4.44	−3.14
$Si_{47}(OH)_{60}$	−5.12	−2.22	2.90	−3.67

nanoclusters exhibit a lower calculated energy gap than that of the nanoclusters of tetrahedral symmetry with the same number of Si atoms.

For the fully passivated Si nanoclusters, we used the B3LYP/6−31G(d)//LDA/SIESTA method to investigate the energy gap and optical properties of alkyl (CH_3−, C_2H_5−, and C_3H_7−), alkenyl (C_2H_3−), oxide (OCH_3− and OH−), nitride (CH_2NH_2− and NH_2−), sulfide (SH− and $(CH_2)_3SH$−), and CN− passivations on the surface of silicon nanoclusters on the basis of the Si_{35} and Si_{47} cores. The B3LYP/6−31G(d)//LDA/SIESTA calculated HOMO, LUMO, energy gaps, and Fermi energy of passivated Si nanoclusters as a function of passivation and core size are shown in Table 4; the relative calculated energy gap as the function of passivants for these passivated Si nanoclusters is shown in Figure 4. To understand the surface passivation effect in the Si nanoclusters, the passivated Si_{35} nanoclusters with different passivants were used for comparison. We observed that the calculated energy gap decreases when the H-passivation is replaced by alkyl, alkenyl, oxide, nitride, or CN− passivation. As shown in Table 4, there are slight differences for the calculated energy gap of alkyl-passivated Si

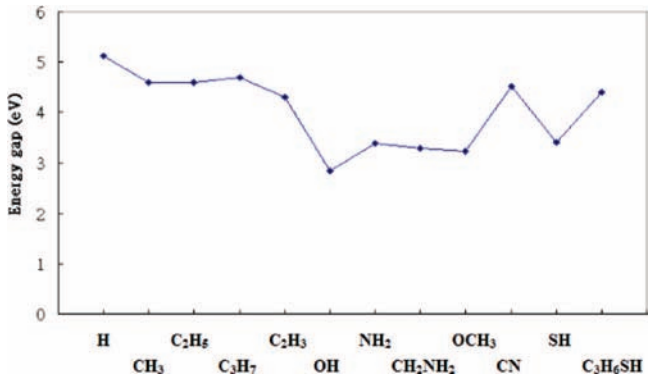

Figure 4. Energy gap of Si_{35} nanoclusters with different passivations.

nanoclusters $Si_{35}(CH_3)_{36}$, $Si_{35}(C_2H_5)_{36}$, and $Si_{35}(C_3H_7)_{36}$. Also, these alkyl-passivated Si nanoclusters have much higher energy gaps than those with oxide shell $Si_{35}(OH)_{36}$, alkoxy shell $Si_{35}(OCH_3)_{36}$, and nitride shell $Si_{35}(NH_2)_{36}$. The trend in the calculated energy gap for the passivated Si_{35} nanoclusters is the following: $Si_{35}H_{36} > Si_{35}(C_3H_7)_{36} > Si_{35}(C_2H_5)_{36} \approx Si_{35}(CH_3)_{36} > Si_{35}(CN)_{36} > Si_{35}(C_3H_6SH)_{36} > Si_{35}(SH)_{36} > Si_{35}(NH_2)_{36} > Si_{35}(CH_2NH_2)_{36} > Si_{35}(OCH_3)_{36} > Si_{35}(OH)_{36}$. In the alkyl-passivated Si nanoclusters, $Si_{35}(CH_3)_{36}$, $Si_{35}(C_2H_5)_{36}$, and $Si_{35}(C_3H_7)_{36}$, the calculated HOMOs increased from −6.80 to −5.43, −5.34, and −5.45 eV while the LUMOs increased from −1.68 to −0.83, −0.75, and −0.75 eV, and the calculated energy gap decreased from 5.12 to 4.60, 4.59, and 4.70 eV with respect to those of $Si_{35}H_{36}$. Our calculations show that the energy gap is reduced by about 0.5 eV when the Si−H bond is replaced by the Si−C bond and thus the effect of alkyl-passivations is rather weak. Recently, Reboredo and Galli reported DFT calculations of the alkyl-terminated Si quantum dots, and then Tanaka et al. confirmed the calculation results by the synchrotron radiation technique.[26,22] They concluded that there is a large red-shift in the absorption spectrum when H is replaced by alkyl passivants and that there is a small change when an additional C atom is added. The calculated LUMO is not very sensitive to the additional C atom on the cluster surface. Our present results are consistent with the previous calculations.[26] $Si_{35}(C_2H_3)$ possesses a C=C alkenyl group, and the calculated LUMO decreases with respect to that with the alkyl passivant. As a result, the calculated energy gap decreases by 0.29 eV as compared to that of $Si_{35}(C_2H_5)$.

In the oxide Si nanocluster $Si_{35}(OH)_{36}$, the calculated HOMO increases to −5.60 eV while the LUMO decreases to −2.75 eV compared to hydrogenated $Si_{35}H_{36}$, and thus, the calculated energy gap increases by about 2.3 eV (5.12 vs 2.84 eV). This calculation result is close to that of Brus's calculation by the DFT method.[25] Pettigrew et al. have reported the experimental result for the alkoxy-passivated Si cluster which shows that oxygen contamination induces a red-shift in the photoluminescence (PL) spectra.[20] A comparison of the calculated optical properties with NH_2− and SH− passivations of the Si_{35} core cluster shows that the calculated HOMOs increase to −4.13 and −6.40 eV while the calculated LUMOs change to −0.74 and −2.99 eV, respectively, and the calculated energy gaps are 3.39 and 3.41 eV for these passivated Si clusters. Particularly, the calculated energy gap for the OH− passivated Si cluster is reduced by about 2.3 eV with respect to that for the hydrogenated Si clusters. For $Si_{35}(CH_2NH_2)_{36}$ and $Si_{35}(C_3H_6SH)_{36}$, we added alkyl CH_2− and C_3H_6− groups on the cluster surface between Si and N, S atoms, respectively, and the calculated energy gap decreased by 0.1 eV and increased by 1 eV relative to those for $Si_{35}(NH_2)_{36}$ and $Si_{35}(SH)_{36}$. Comparing the calculated energy gaps with oxide, nitride, and sulfide passivations of $Si_{35}H_{36}$, we can see that they decrease. Theoretically, the oxide and sulfide passivations generate a specific chemical interaction (partial double bonding between Si and C or S), which pushes the HOMO up and the LUMO down. Recently, the electronic structure and luminescence properties of oxide, hydrogen, and alkyl-passivated Si nanoclusters were calculated by the DFT method.[14,15] Experimentally, the hydrogenated Si nanocluster emits above 3.0 eV in the blue, whereas it would emit near 2.0 eV in the yellow−red when oxidized.[34,35] Thus, the oxide and sulfide passivations should generate a red-shift in luminescence spectra relative to hydrogenated Si clusters. Our calculation results for OH passivation are consistent with those of Zhou et al. and Puzder et al.[23,25]

Zhou et al. mentioned that the HOMO energy level is related to the formation of a dipole on the surface of the cluster.[24] The relative tendency to form a polar bond is characterized by the index of electronegativity: H = 2.1 eV, C = 2.5 eV, N = 3.0 eV, O = 3.5 eV, S = 2.58 eV, and Si = 1.9 eV.[36] Thus, the passivatants used in this study are all electron-withdrawing groups with respect to the Si atom; all of the calculated HOMO levels for the Si_{35} core-passivated nanoclusters are lower than that of $Si_{35}H_{36}$. We calculated the dipole moment of the substituent on the surface of Si cluster; C_3H_7−, C_2H_5−, and CH_3− have very similar dipole moments, and thus they have close calculated HOMO energies. Comparing CN− versus H− passivation, we can see that the calculated HOMO, LUMO, and Fermi energy decreased to −9.17, −4.65, and −6.91 eV versus −6.80, −1.68, and −4.24 eV, respectively. Since the electron-withdrawing CN− passivatants are located on the cluster surface and contain the triple bond between C and N, the influence on the calculated HOMO and LUMO is apparent; these values drop to −9.17 eV and −4.65 eV, respectively. Recently, Zhou et al. reported the DFT calculated HOMO, LUMO, and energy gap of the Si_{35} cluster with H and F passivations.[24] They concluded that a major effect of the polar Si−F surface bonding is to increase the surface dipole and thus to lower the Fermi energy with respect to H passivation, since F is very strongly electronegative.

Theoretically, the surface dipole might also affect the Fermi energy of passivated silicon nanoclusters. For the Si_{35} species, the calculated Fermi energy decreases from −2.44 eV ($Si_{35}(NH_2)_{36}$) to −6.91 eV ($Si_{35}(CN)_{36}$). Electron-withdrawing OH and CN passivants increase the surface dipole and lower the Fermi energy level for $Si_{35}(OH)_{36}$ and $Si_{35}(CN)_{36}$. Both HOMO and LUMO shift toward negative values, but the shift is not equal; the LUMO negative shifts are larger than those for HOMO, and thus, the energy gap decreases with respect to that of $Si_{35}H_{36}$. For alkyl-passivated Si_{35} clusters, alkyl passivations (CH_3−, C_2H_5−, and C_3H_7−) decrease the surface dipole and increase the Fermi energy and so they have very similar calculated Fermi energy. We conclude that the calculated Fermi energy for passivated Si nanoclusters is passivant dependent.

To investigate the passivation effect on the surface of Si clusters with different core sizes, we compared the different core size Si nanoclusters with CH_3− passivation; the calculated energy gap of $Si_{35}(CH_3)_{36}$ is 0.16 and 0.66 eV higher than those of $Si_{47}(CH_3)_{60}$ and $Si_{20}(CH_3)_{20}$, respectively. Since the $Si_{20}(CH_3)_{20}$ cluster with I_h symmetry is subject to quantum confinement, it exhibits a lower calculated energy gap than that of the tetrahedral Si nanocluster with the same core size.

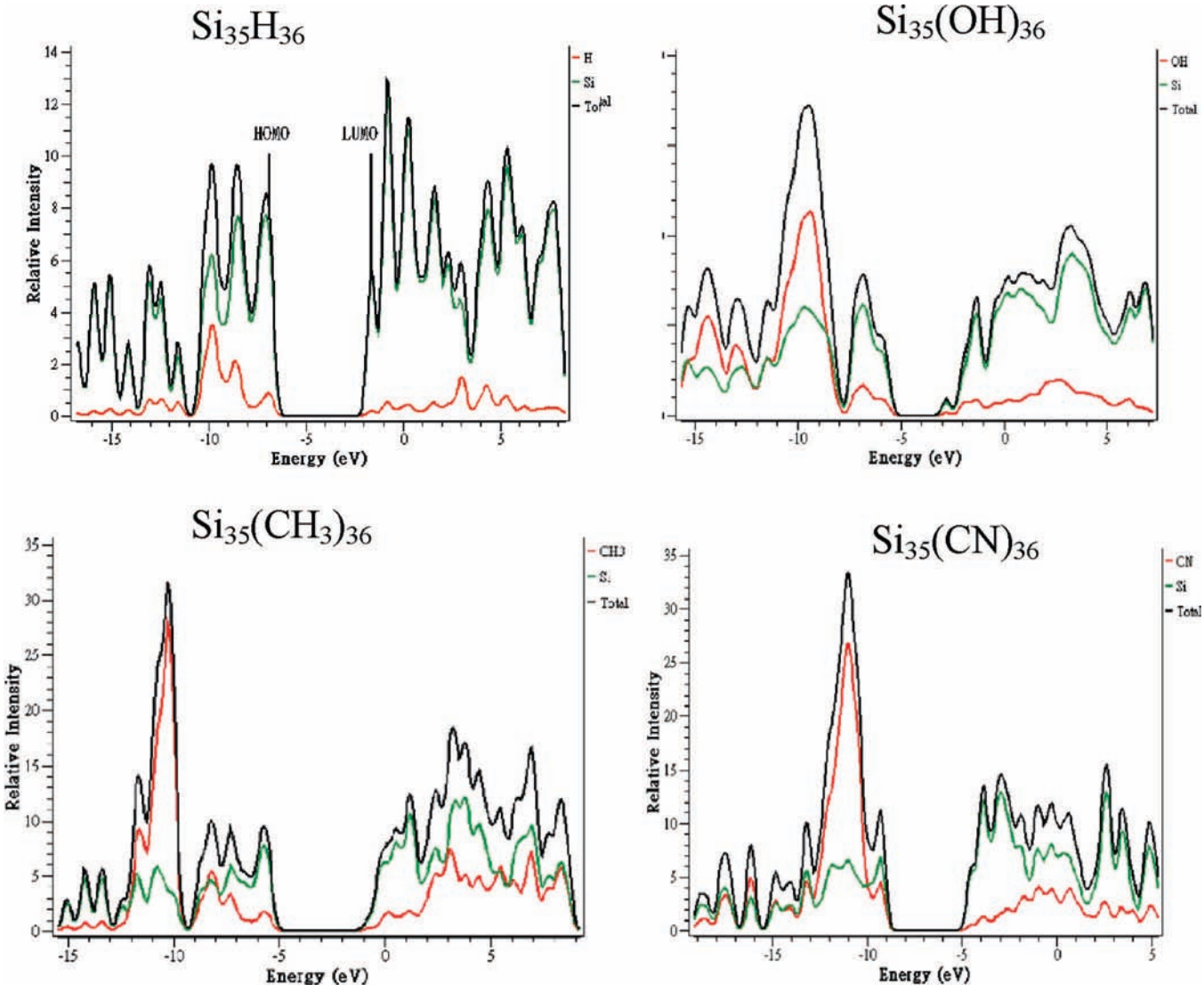

Figure 5. Calculated TDOS and PDOS of the $Si_{35}H_{36}$, $Si_{35}(OH)_{36}$, $Si_{35}(CH_3)_{36}$, and $Si_{36}(CN)_{36}$ clusters.

Information regarding the HOMO and LUMO can also be obtained from Figure 5, which shows the calculated total density of states (TDOS) and projected density of states (PDOS) of the Si core clusters with H, OH, CH_3, and CN passivants, in particular for $Si_{35}H_{36}$, $Si_{35}(CH_3)_{36}$, $Si_{35}(OH)_{36}$, and $Si_{35}(CN)_{36}$ clusters. Figure 5 shows sharper features for the molecular-like passivated Si clusters than those of Si bulk.[32] The atoms associated with HOMO are likely to give up electrons when excited. The band diagram of $Si_{35}H_{36}$ showed a broad band between −6 and −11 eV and the Si−H bonding peak around −10 eV. We can see that the HOMO and LUMO energy levels of $Si_{35}H_{36}$, $Si_{35}(CH_3)_{36}$, and $Si_{35}(OH)_{36}$ are mainly composed of the TDOS of Si atoms. Si and CN give equal contributions to the HOMO, and the Si core mainly contributes to the LUMO for $Si_{35}(CN)_{36}$. For $Si_{35}(CH_3)_{36}$, $Si_{35}(OH)_{36}$, and $Si_{35}(CN)_{36}$, the valence and conducting bands are mainly composed from contributions of the passivant and the Si core orbitals, respectively.

According to our previous calculations, we conclude that the calculated energy gap of Si nanocluster is core size dependent and decreases when the size increases. Thus, the calculated energy gaps of $Si_{47}(CH_3)_{60}$ and $Si_{47}(OH)_{60}$ are 0.16 and 0.07 eV lower than those of $Si_{35}(CH_3)_{36}$ and $Si_{35}(OH)_{36}$, respectively.

Conclusion

The LDA/SIESTA, B3LYP/6−31G(d)//LDA/SIESTA, AM1//LDA/SIESTA, PM3//LDA/SIESTA, AM1, PM3, B3LYP/6−31G(d), and B3LYP/LANL2DZ calculations have been applied to investigate the energy gaps and optimized structures of hydrogenated silicon nanoclusters ranging from Si_5H_{12} to $Si_{281}H_{172}$ for T_d symmetry and $Si_{20}H_{20}$ to $Si_{100}H_{60}$ for I_h symmetry. It is found that the calculated energy gap in the ground state decreases as the cluster size increases. We also conclude that the calculated energy gap is underestimated for these Si nanoclusters by the LDA/SIESTA calculation. The energy gaps obtained by the B3LYP/6−31G(d)//LDA/SIESTA and B3LYP/6−31G(d) methods are close to each other. Similarly, the calculated results by AM1 and PM3, AM1//LDA/SIESTA, and PM3//LDA/SIESTA are close for both sets. The pseudopotential B3LYP/LANL2DZ calculations overestimate the energy gap. A plot of the energy gap versus $1/d(N_{si})$ could generate the energy gap of bulk Si material (Figure 2), and thus the energy gaps calculated by DFT methods (including B3LYP/6−31G(d) and B3LYP/6−31G(d)//LDA/SIESTA) are close to the experimental value for bulk material. Since the calculation in the passivated Si nanoclusters require very large computing demands, we proposed that the B3LYP/6−31G(d)//LDA/

SIESTA method with the 6−31G(d) basis set is an appropriate approach to determine optical properties of Si nanoclusters with different passivants. For the fully passivated silicon nanoclusters, the CH_3-, CH_2CH_3-, and $CH_2CH_2CH_3-$ alkyl passivants affect the calculated energy gap weakly, whereas the cluster energy gap increases because of the electron-withdrawing OH− and NH_2- passivations. The strong electron-withdrawing CN− passivant decreases the calculated HOMO, LUMO, and Fermi energy compared to that of hydrogenated Si cluster. For passivated Si nanoclusters with different passivants, we found that they may influence the calculated Fermi energy. The core size effect for passivated Si nanoclusters is the same as that in hydrogenated Si nanoclusters.

Acknowledgment. We thank Prof. Alexander Mebel for reading the manuscript, the National Science Council of Taiwan for financial support, and the National Center for High-performance Computing in Hsinchu for providing access to the computational resources.

References and Notes

(1) Schmedake, T. A.; Cunin, F.; Link, J.; Sailor, M. *Adv. Mater.* **2002**, *14*, 1270.
(2) Dubertret, B.; Skourides, P.; Norris, D. J.; Noireaux, V. H. B. A.; Libchaber, A. *Science* **2002**, *298*, 1759.
(3) Manna, L.; Scher, E.; Alivisatos, A. *J. Am. Chem. Soc.* **2000**, *122*, 12700.
(4) Green, M. *Angew. Chem., Int. Ed.* **2004**, *43*, 4129.
(5) Warner, J. H.; Hoshino, A.; Yamamoto, K.; Tilley, R. D. *Angew. Chem., Int. Ed.* **2005**, *44*, 4550.
(6) Ögüt, S.; Chelikowsky, J. R. *Phys. Rev. Lett.* **1997**, *79*, 1770.
(7) Vasiliev, I.; Ögüt, S.; Chelikowsky, J. R. *Phys. Rev. Lett.* **2001**, *86*, 1813.
(8) Wolkin, M. V.; Jorne, J.; Fauchet, P. M.; Allan, G.; Delerue, C. *Phys. Rev. Lett.* **1999**, *82*, 197.
(9) Rohlfing, M.; Louie, S. G. *Phys. Rev. Lett.* **1998**, *80*, 3320.
(10) Franceschetti, A.; Wang, L. W.; Zunger, A. *Phys. Rev. Lett.* **1999**, *83*, 1269.
(11) Yang, J. C.; Bai, X.; Li, C. P.; Xu, W. G. *J. Phys. Chem. A* **2005**, *109*, 5717.
(12) Wilcoxon, J. P.; Samara, G. A.; Provencio, P. N. *Phys. Rev. B* **1999**, *60*, 2704.
(13) Garoufalis, C. S.; Zdetsis, A. D. *Phys. Rev. Lett.* **2001**, *87*, 276402-1.
(14) Rohlfing, M.; Louie, S. G. *Phys. Rev. Lett.* **1998**, *80*, 3320.
(15) Belkhir, M. A.; Mahtout, S.; Belabbas, I.; Samah, M. *Physica E* **2006**, *31*, 86.
(16) Williamson, A. J.; Grossman, J. C.; Hood, R. Q.; Puzder, A.; Galli, G. *Phys. Rev. Lett.* **2002**, *89*, 196803-1.
(17) Reboredo, F. A.; Franceschetti, A.; Zunger, A. *Phys. Rev. B* **2000**, *61*, 13073.
(18) Wang, X.; Zhang, R. Q.; Lee, S. T.; Niehaus, T. A.; Frauenheim, T. H. *Appl. Phys. Lett.* **2007**, *90*, 123116-1.
(19) Li, X. G.; Hey, Q.; Swihart, M. T. *Langmuir* **2004**, *20*, 4720.
(20) Pettigrew, K. A.; Liu, Q.; Power, P. P.; Kauzlarich, S. M. *Chem. Mater.* **2003**, *15*, 4005.
(21) Larson, D. R.; Zipfel, W. R.; Williams, R. M.; Clark, S. W.; Bruchez, M. P.; Wise, F. W.; Webb, W. W. *Science* **2003**, *300*, 1434.
(22) Tanaka, A.; Saito, R.; Kamikake, T.; Imamura, M.; Yasuda, H. *Eur. Phys. J. D* **2007**, *43*, 229.
(23) Puzder, A.; Williamson, A. J.; Reboredo, F. A.; Galli, G. *Phys. Rev. Lett.* **2003**, *91*, 157405-1.
(24) Zhou, Z.; Friesner, R. A.; Brus, L. *J. Am. Chem. Soc.* **2003**, *125*, 15599.
(25) Zhou, Z.; Brus, L.; Friesner, R. *Nano Lett.* **2003**, *3*, 163.
(26) Reboredo, F. A.; Galli, G. *J. Phys. Chem. B* **2005**, *109*, 1072.
(27) Vasilliev, I. *Phys. Status Solidi* **2003**, *239*, 19.
(28) Zhao, Y.; Kim, Y. H.; Du, M. H.; Zhang, S. B. *Phys. Rev. Lett.* **2004**, *93*, 015502-1.
(29) (a) Ordejón, P.; Artacho, E.; Soler, J. M. *Phys. Rev. B* **1996**, R10441. (b) Sánchez-Portal, D.; Ordejón, P.; Artacho, E.; Soler, J. M. *Int. J. Quantum Chem., Quantum Chem. Symp.* **1997**, *65*, 453. (c) Soler, J. M.; Artacho, E.; Gale, J. D.; Garcia, A.; Junqquera, J.; Ordejón, P.; Sánchez-Portal, D. *J. Phys: Condens. Matter* **2002**, *14*, 2745.
(30) (a) Perdew, J. P.; Zunger, A. *Phys. Rev. B* **1981**, *23*, 5048. (b) Perdew, J. P.; Burke, K.; Wang, Y. *Phys. Rev. B* **1996**, *54*, 16533.
(31) Frisch, M. J.; Trucks, G. W.; Schlegel, H. B.; Scuseria, G. E.; Robb, M. A.; Cheeseman, J. R.; Zakrzewski, V. G.; Montgomery, J. A.; Stratmann, R. E.; Burant, J. C.; Dapprich, S.; Millam, J. M.; Daniels, A. D.; Kudin, K. N.; Strain, M. C.; Farkas, O.; Tomasi, J.; Barone, V.; Cossi, M.; Cammi, R.; Mennucci, B.; Pomelli, C.; Adamo, C.; Clifford, S.; Ochterski, J.; Petersson, G. A.; Ayala, P. Y.; Cui, Q.; Morokuma, K. D.; Malick, K.; Rabuck, A. D.; Raghavachari, K.; Foresman, J. B.; Cioslowski, J.; Ortiz, J. V.; Stefanov, B. B.; Liu, G.; Liashenko, A. P.; Piskorz, K. I.; Gomperts, R.; Martin, R. L.; Fox, D. J.; Keith, T.; Al-Laham, M. A.; Peng, C. Y.; Nanayakkara, A.; Gonzalez, C.; Challacombe, M.; Gill, P. M. W.; Johnson, B. G.; Chen, W.; Wong, M. W.; Andres, J. L.; Head-Gordon, M.; Replogle, E. S.; Pople, J. A. *Gaussian 03*; Gaussian, Inc.: Pittsburgh, PA, 2003.
(32) Zunger, A.; Wang, L. W. *Appl. Surf. Sci.* **1996**, *102*, 350.
(33) Hill, N. A.; Whaley, K. B. *Phys. Rev. Lett.* **1995**, *75*, 1130.
(34) Puzder, A.; Williamson, A. J.; Grossman, J. C.; Galli, G. *Phys. Rev. Lett.* **2002**, *88*, 097401-1.
(35) Vasiliev, I.; Chelikowsky, J. R.; Martin, R. M. *Phys. Rev. B* **2002**, *65*, 121302-1.
(36) Atkins, P.; Paula, J. D. *Physical Chemistry*, 8th ed.; Oxford University Press: Oxford, UK, 2006.

JP8006975